SUPPLEMENTAL DATA

CHARACTERIZATION OF LipL AS A NON-HEME, Fe(II)-DEPENDENT α-KETOGLUTARATE:UMP DIOXYGENASE THAT GENERATES URIDINE-5'-ALDEHYDE DURING A-90289 BIOSYNTHESIS

Zhaoyong Yang[a], Xiuling Chi[a], Masanori Funabashi[b], Satoshi Baba[b], Koichi Nonaka[b], Pallab Pahari[a], Jason Unrine[c], Jesse M. Jacobsen[a], Gregory I. Elliott[a], Jürgen Rohr[a], and Steven G. Van Lanen[a,1]

[a]Department of Pharmaceutical Sciences, College of Pharmacy, University of Kentucky, 789 S. Limestone, Lexington, KY 40536, USA
[b]Biopharmaceutical Research Group I, Biopharmaceutical Technology Research Laboratories, Pharmaceutical Technology Division, Daiichi Sankyo Co., Ltd., 389-4, Aza-ohtsurugi, Shimokawa, Izumi-machi, Iwaki-shi, Fukushima 971-8183, Japan
[c]Department of Plant and Soil Sciences, College of Agriculture, University of Kentucky, Lexington, KY 40536, USA

Supplemental Methods

2',3'-*O*-*p*-Methoxybenzylideneuridine: To a solution of uridine (2.0 g, 8.2 mmol) in dry THF (30 mL), $ZnCl_2$ (1.1 g, 8.2 mmol) and *p*-methoxybenzaldehyde (4 mL, 32.8 mmol) was added. The turbid mixture was stirred for 2 days at room temperature and THF was removed. Product was precipitated by the addition of diethyl ether (50 mL), which was filtered, washed with water (2 × 25 mL) and diethyl ether (2 × 25 mL). Crystallization from hot water containing a little ethanol provided 2',3'-*O*-*p*-methoxybenzylideneuridine (2.1 g, 71%) as white solid. Mp: 205-206 °C (lit: 207-208 °C) (1). ^{1}HNMR (DMSO-d_6, 500 MHz) (2): δ 11.40 (brs, 1H), 7.83 and 7.75 (2 × d, 1H, J = 8.0 Hz), 7.45 and 7.40 (2 × d, 2H, J = 8.5 Hz), 6.98 and 6.96 (2 × d, 2H J = 9.0 Hz), 6.06 and 5.92 (2 × s, 1H), 5.95 (2 × d, 1H, J = 3.0 Hz), 5.65 (2 × dd, 1H, J = 8.0, 2.0 Hz), 5.13 and 5.09 (2 × brs, 1H), 4.99 and 4.97 (2 × dd, 1H, J = 6.5, 2.5 Hz), 4.87 and 4.82 (2 × dd, 1H, J = 6.5, 3.0 Hz), 4.24 and 4.15 (2 × dd, 1H, J = 4.5, 3.5 Hz), 3.78 and 3.77 (2 × s, 3H), 3.65 and 3.61 (2 × m, 2H).

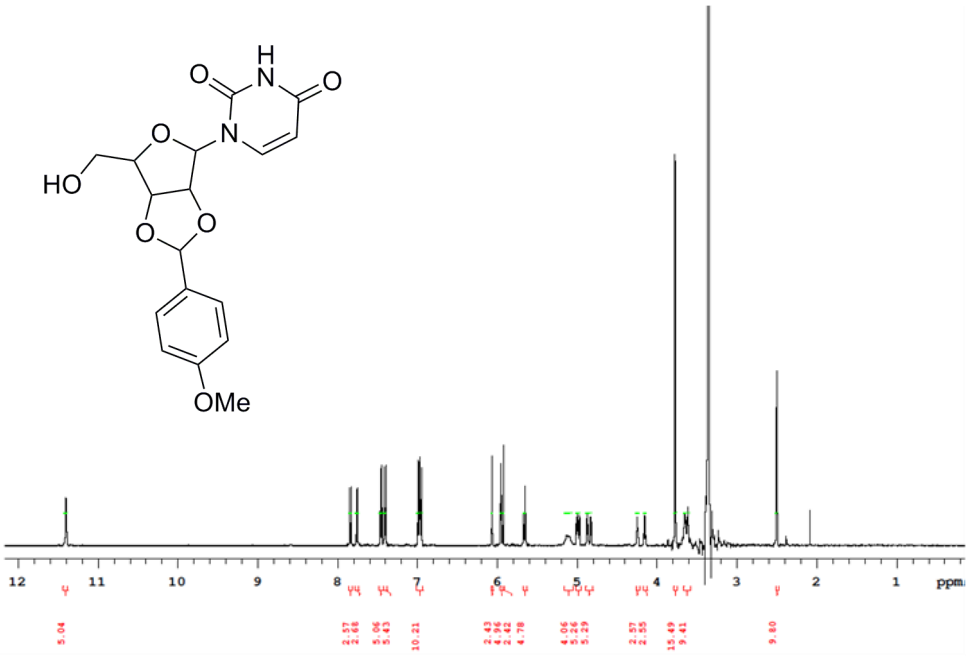

Uridine 5'-aldehyde: Trifluoroacetic acid (0.2 mL, 2.5 mmol) was added to an ice-cooled solution of 2',3'-*O*- *p*-methoxybenzylideneuridine (1.0 g, 2.76 mmol), *N*,*N*'-dicyclohexylcarbodiimide (3.1 g, 15 mmol), and pyridine (0.04 mL, 5 mmol) in anhydrous dimethyl sulfoxide (13 mL), and the resulting mixture was stirred at room temperature for 16 h. Ethyl acetate (50 mL) was added to the reaction mixture and precipitated *N*,*N*'-Dicyclohexylurea was filtered off while washing with another portion of ethyl acetate (50 mL). Combined filtrates were washed with water (2 × 50 mL), dried (Na_2SO_4), and concentrated to give crude 2',3'-*O*-*p*-methoxybenzylideneuridine 5'-aldehyde as a white solid. Without further purification, the compound was dissolved in a solution of 90% trifluoroacetic acid (20 mL) and stored at 37 °C for 16 h and then concentrated. An aqueous solution (30 mL) of the residue was washed with chloroform (2 × 15 mL) and ethyl acetate (20 mL). Removal of the water afforded compound uridine-5'-aladehyde (360 mg, 54% in two steps) as off-white foam. The compound is extremely hygroscopic in nature and exists mostly in hydrated form (Fig. S7). ^{1}HNMR (D_2O, 500 MHz) (3): δ 7.88 (d, 1H, J = 8.0 Hz), 5.96 (d, 1H, J = 6.0 Hz), 5.88 (d, 1H, J = 8.0 Hz), 5.17 (d, 1H, J = 4.0 Hz), 4.37 (dd, 1H, J = 6.0, 5.5 Hz), 4.32-4.26 (1H, m), 4.00 (dd, 1H, J = 4.0, 3.5 Hz); ^{13}CNMR (D_2O, 125 MHz): δ 166.05, 151.74, 141.88, 102.44, 88.53, 86.17, 73.26, 69.60.

Supplemental References

1. Smith, M., Rammler, D. H., Goldberg, I. H., and Khorana, H. G. (1962) *J. Am. Chem. Soc.* **84**, 430-440
2. Brunschweiger, A., Iqbal, J., Umbach, F., Scheiff, A. B., Munkonda, M. N., Sévigny, J., Knowles, A. F., and Müller, C. E. (2008) *J. Med. Chem.* **51**, 4518–4528
3. Jones, G. H., Taniguchi, M., Tegg, D., Moffatt, J. G. (1979) *J. Org. Chem.* **44**, 1309-1317

Supplemental Figures

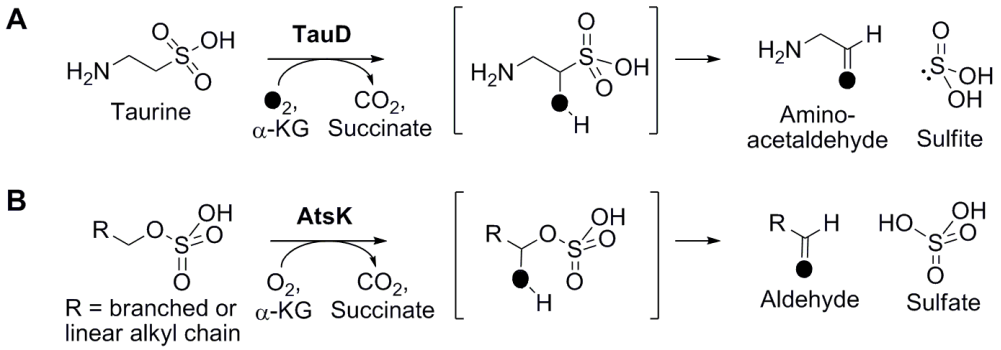

Fig. S1. Reactions catalyzed by representative Fe(II)- and α-KG-Dependent Dioxygenases. (*A*) The reaction catalyzed by α-KG:taurine dioxygenase (TauD) depicting the proposed incorporation of an oxygen atom from dioxygen into the aldehyde product. (*B*) The reaction catalyzed by AtsK, also depicting the proposed incorporation of an oxygen atom from dioxygen into the aldehyde product.

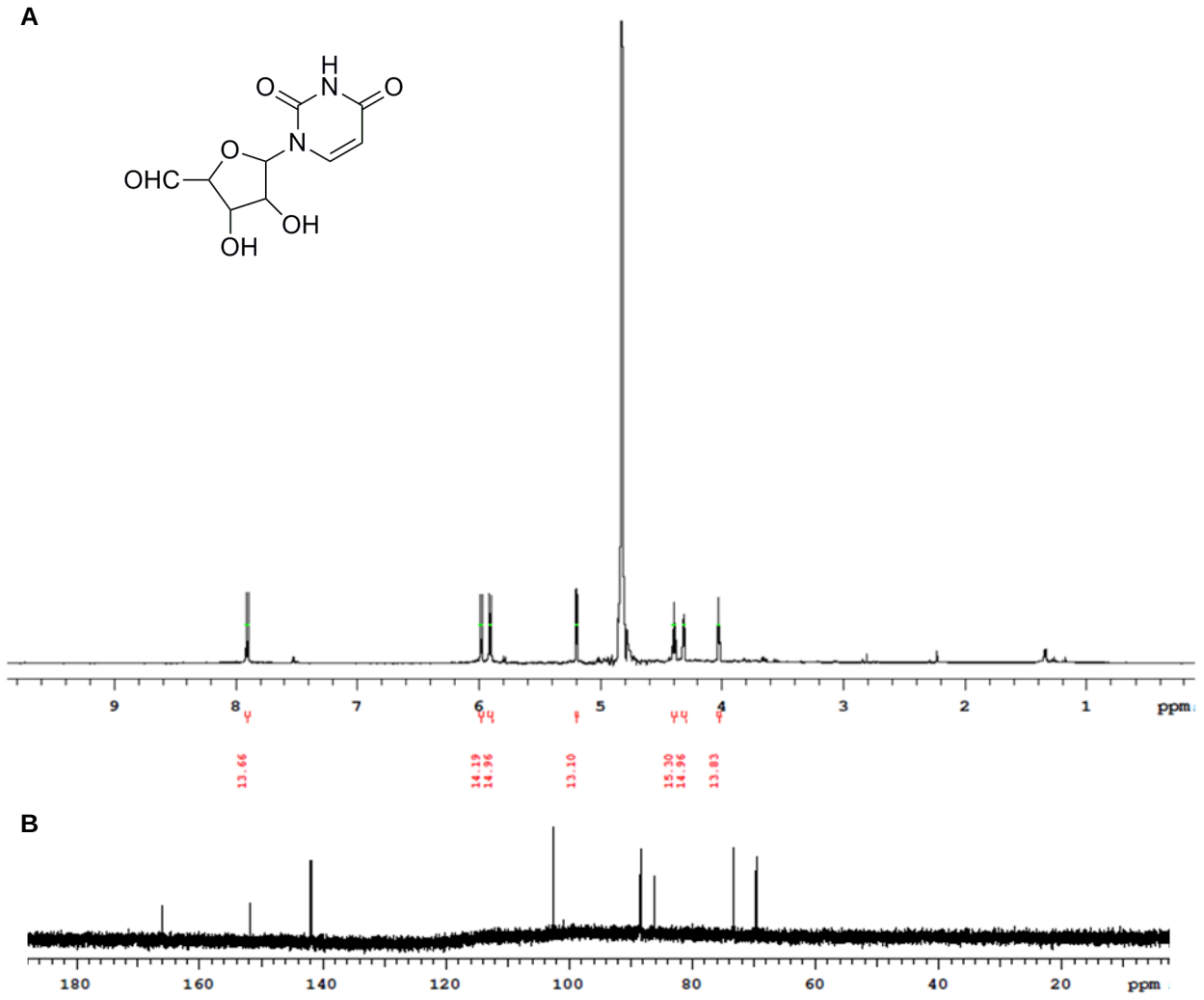

Fig. S2. Spectroscopic analysis of synthetic uridine-5'-aledehyde. (*A*) ^{1}H-NMR spectrum in D_2O and (*B*) ^{13}C-NMR spectrum.

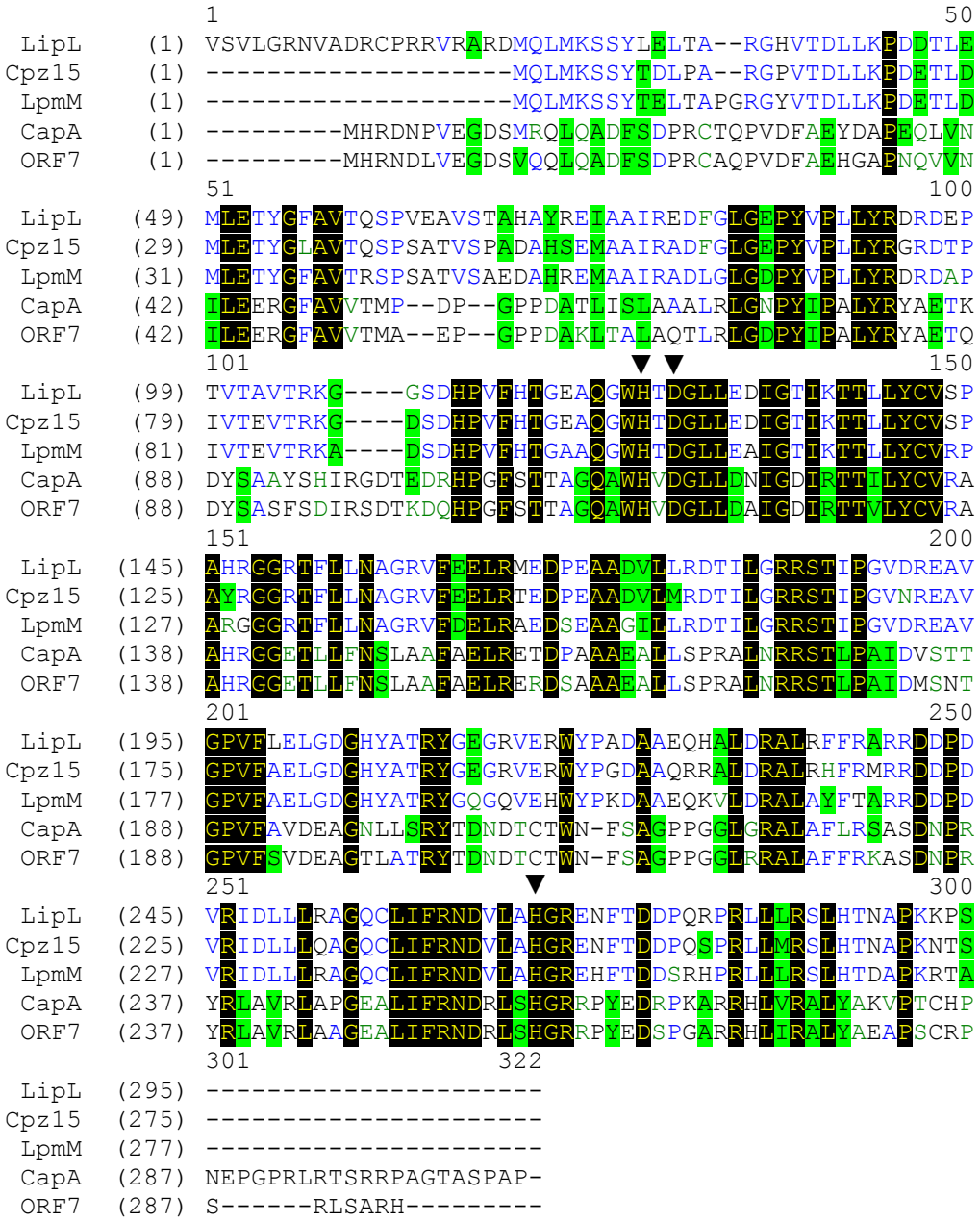

Fig. S3. Bioinformatics analysis of LipL. Sequence alignment of LipL with homologous enzymes from the gene clusters involved in the biosynthesis of high-carbon nucleoside antibiotics including Cprz15 from the caprazamycin gene cluster, LpmM from the liposidomycin gene cluster, CapA from the A-503083 gene cluster, and ORF7 from the A-500359 gene cluster. Conserved residues predicted to be involved in Fe(II) binding are indicated (▼).

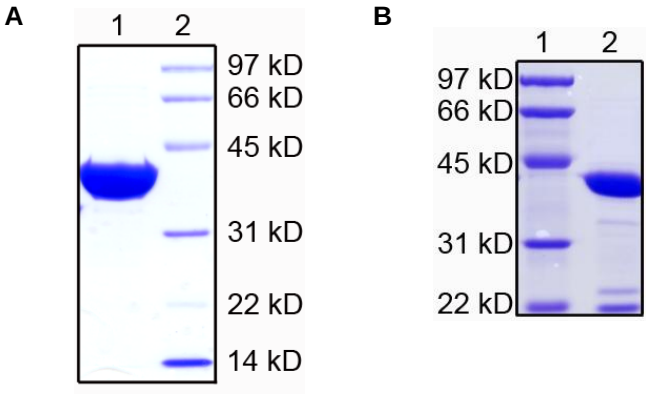

Fig. S4. Purification of recombinant dioxygenases from *E. coli*. (*A*) SDS-PAGE of purified His_6-LipL (expected 38.2 kD). (*B*) SDS-PAGE of purified His_6-*Ec*TauD (expected 37.4 kD). The engineered N-terminal His_6-tag contributes approximately 5 kD to the native molecular mass.

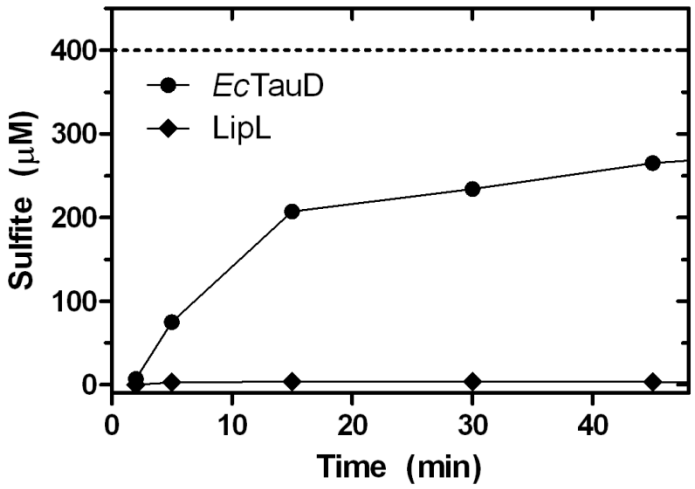

Fig. S5. Time course of dioxygenase activity by detection of sulfite. The maximal amount of product is indicated by the dashed (---) line.

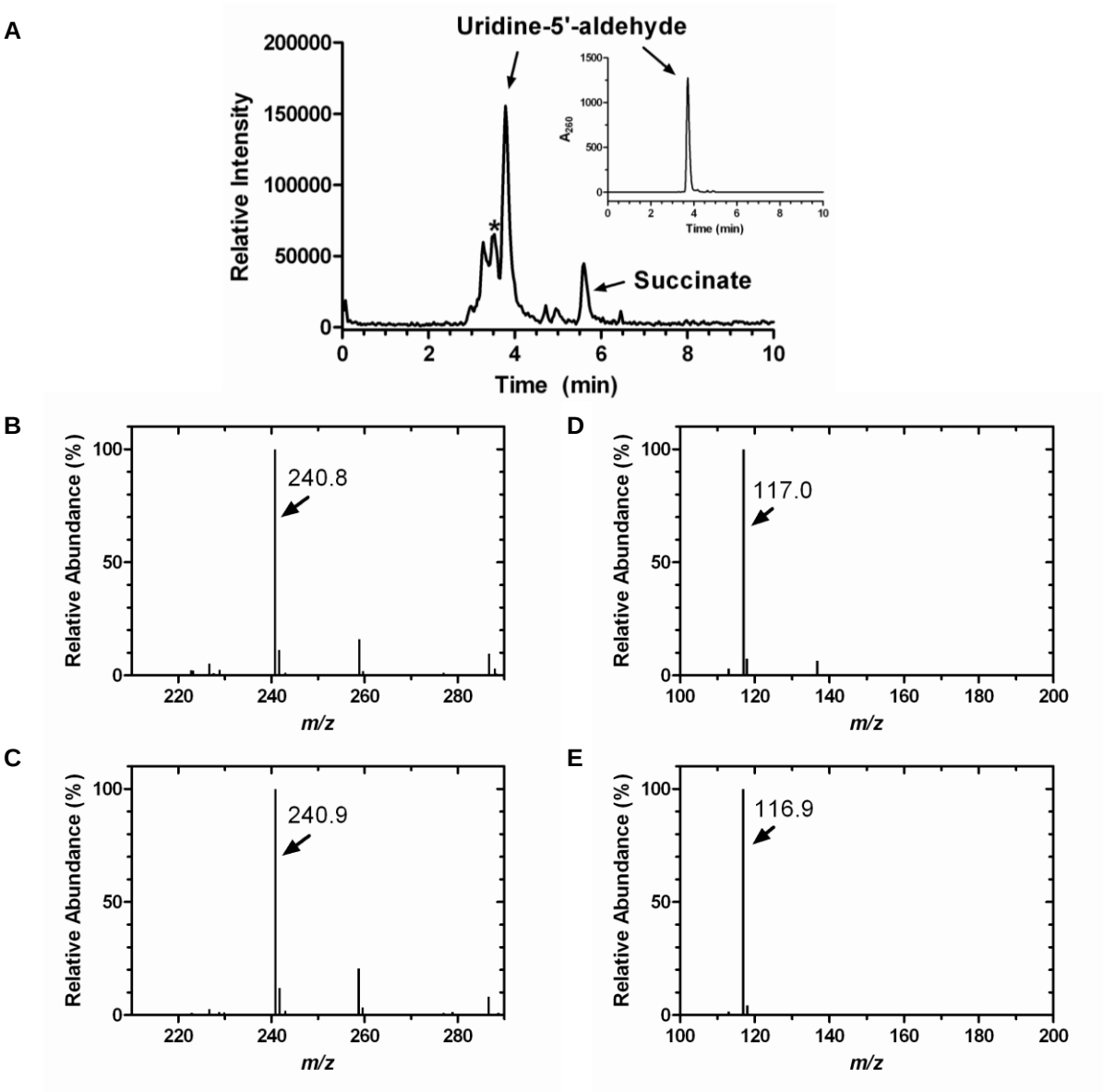

Fig. S6 LC-MS analysis of the LipL-catalyzed reaction (*A*) The reaction components were detected by total negative ion current and UV/Vis spectroscopy (inset). The asterisks (*) denotes an unidentified peak with the similar retention time as UMP but distinct mass. (*B*) Mass spectrum for the peak at elution time t = 3.8 min corresponding to uridine-5'-aldehyde. (*C*) Mass spectrum for authentic uridine-5'-aldehyde. (*D*) Mass spectrum for the peak at elution time t = 5.6 min corresponding to succinate. (*E*) Mass spectrum of authentic succinate. A_{260}, absorbance at 260 nm.

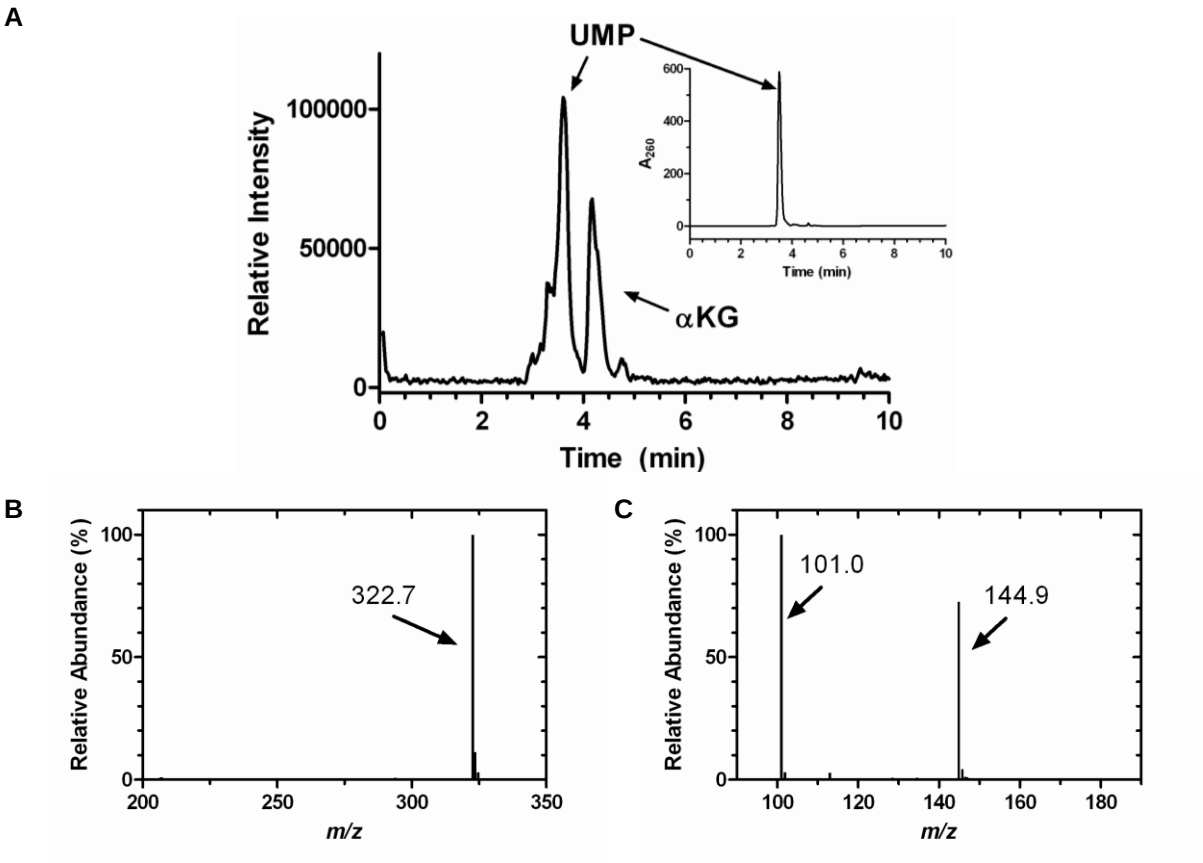

Fig. S7. LC-MS analysis of control reactions. (*A*) The reaction components were detected by total negative ion current and UV/Vis spectroscopy (inset). (*B*) Mass spectrum for the peak at elution time t = 3.5 min corresponding to UMP. (*C*) Mass spectrum for the peak at elution time t = 4.2 min corresponding to α-KG. A_{260}, absorbance at 260 nm.

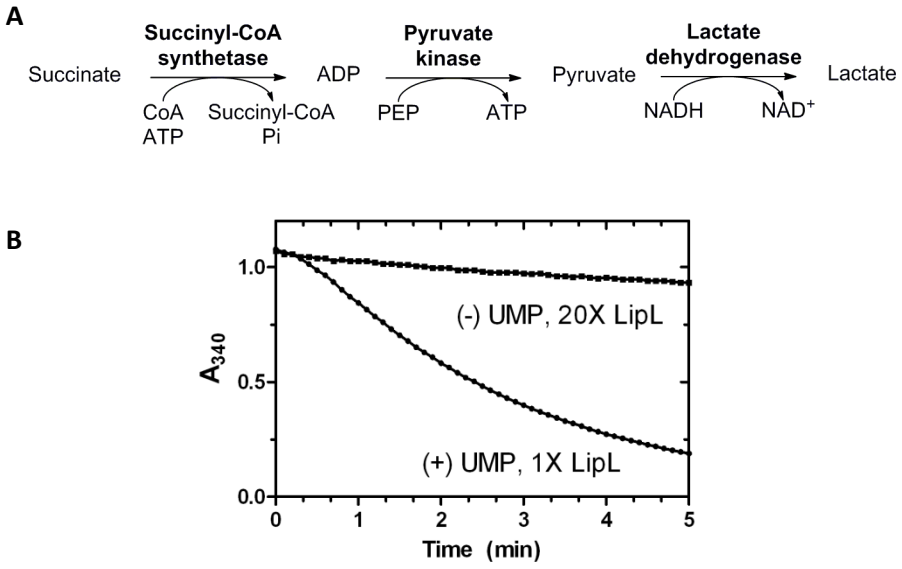

Fig. S8. Detection of succinate production using an enzyme coupled reaction. (*A*) Scheme depicting the reactions catalyzed by the three additional enzymes that leads to oxidation of NADH for detection by UV/Vis spectroscopy. (*B*) The LipL-catalyzed reaction with or without the addition of UMP. In the absence of UMP, significantly more enzyme was required to detect activity. A_{340}, absorbance at 340 nm.

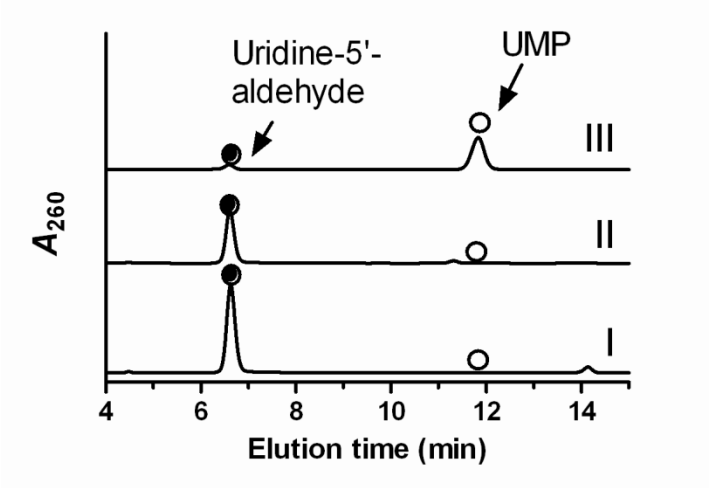

Fig. S9. Requirement of dioxygen for LipL activity. The reaction was performed with LipL in an open atmosphere (I), a saturated O_2 atmosphere (II), or saturated N_2 atmosphere (III). In all cases, the reaction mixture was degassed with argon prior to the addition of enzyme. A_{260}, absorbance at 260 nm.

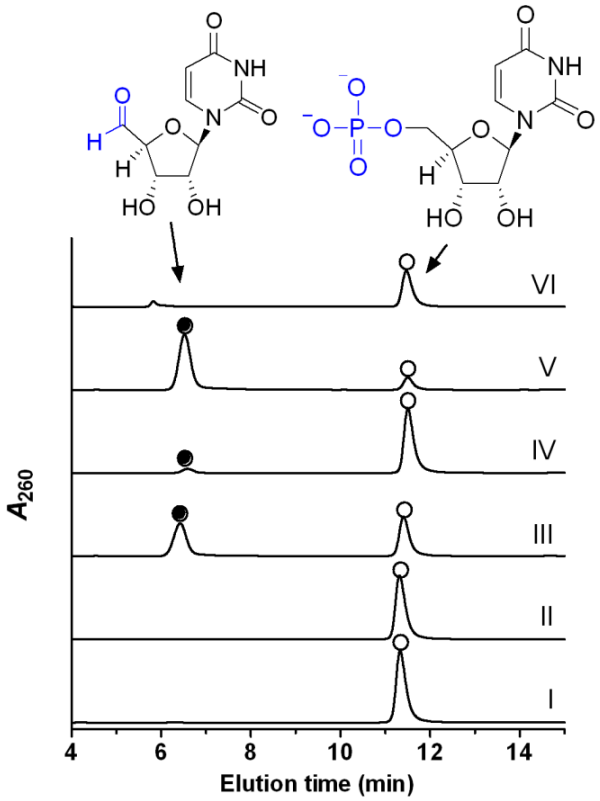

Fig. S10. Requirements for LipL activity. Analysis of the LipL reaction using UMP as the prime substrate with the omission of enzyme (I), α-ketoglutarate (II), ferrous iron (III), or ascorbate (IV), and the reaction containing all of the components without (V) or with EDTA (VI). UMP (○) and uridine-5'-aldehyde (●); A_{260}, absorbance at 260 nm.

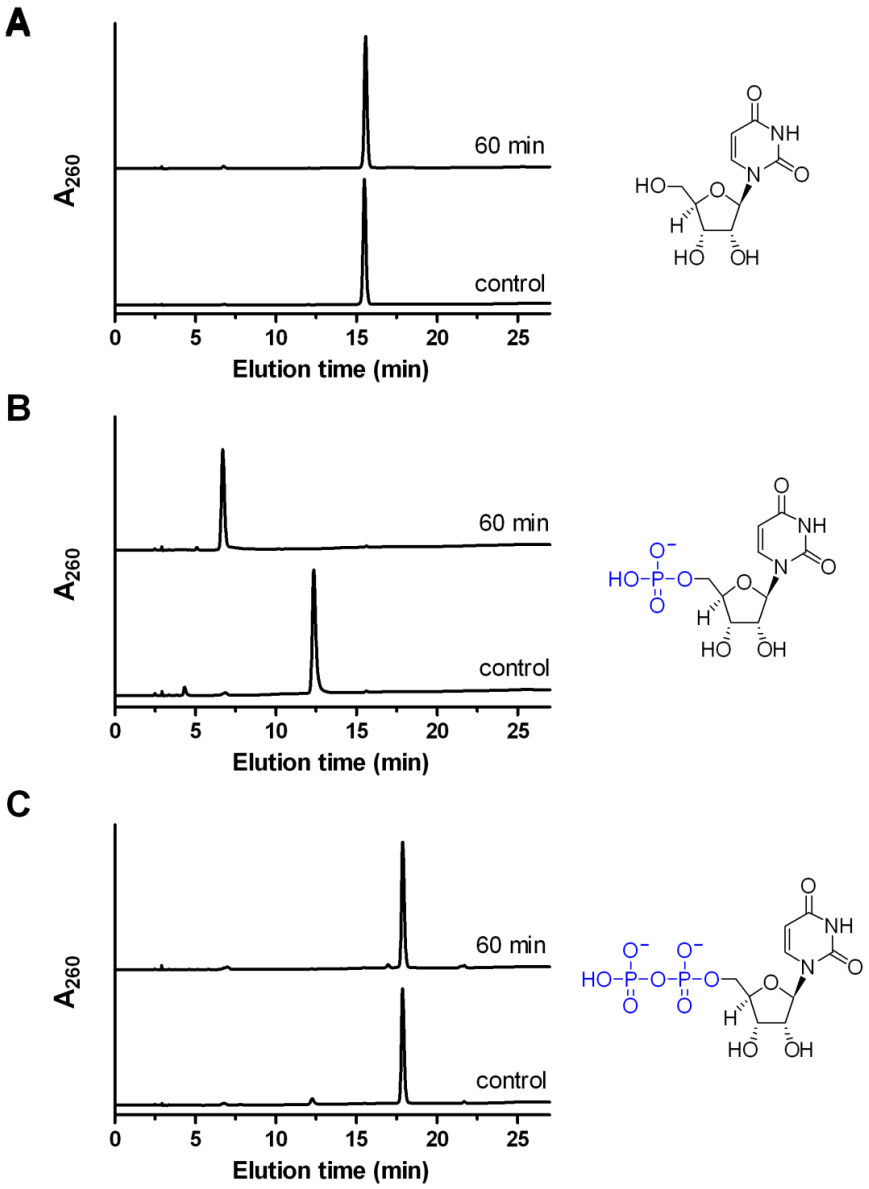

Fig. S11. Activity of LipL with uridine nucleoside and nucleotides. The LipL-catalyzed reaction was performed with (*A*) uridine, (*B*) UMP, or (*C*) UDP. Control reactions were run without enzyme. A_{260}, absorbance at 260 nm.

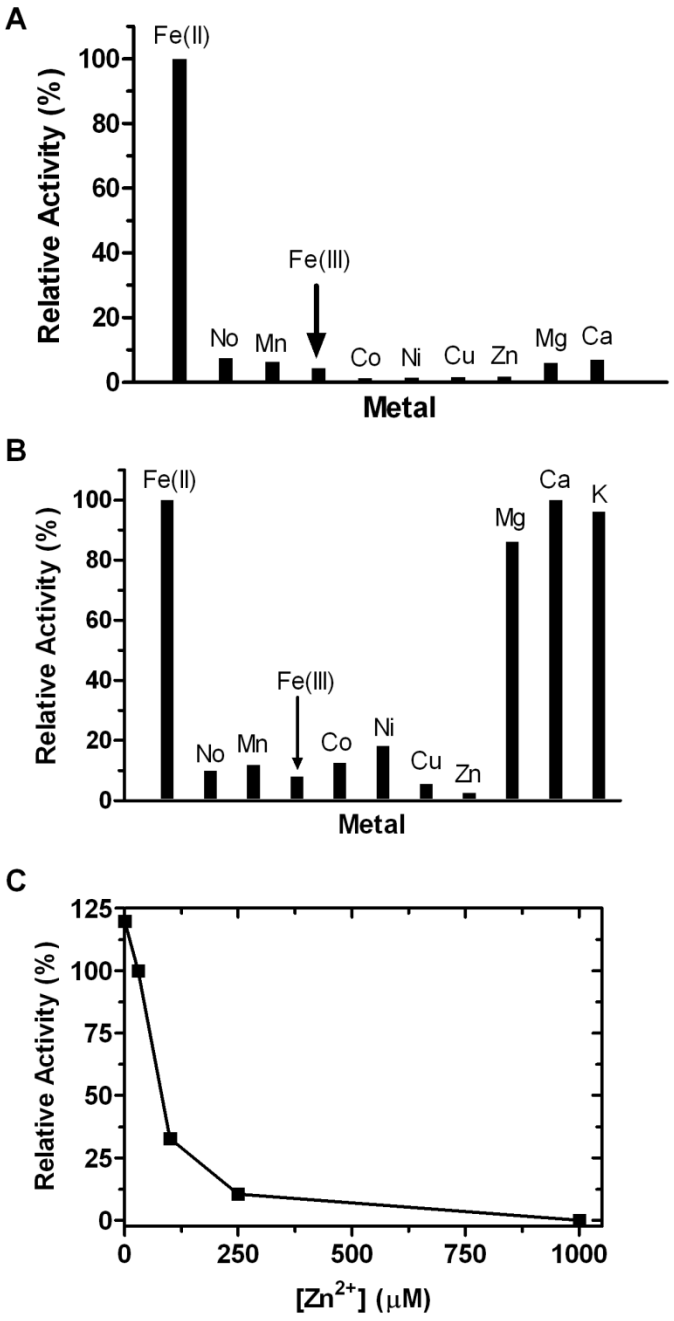

Fig. S12. Effect of metals on LipL activity. (*A*) The indicated metal substituted Fe(II) using the standard reaction conditions. (*B*) The indicated metal was included with equimolar concentrations of Fe(II) using the standard reaction conditions. (*C*) Activity with the addition of Zn^{2+} using the optimized reaction conditions for each enzyme.

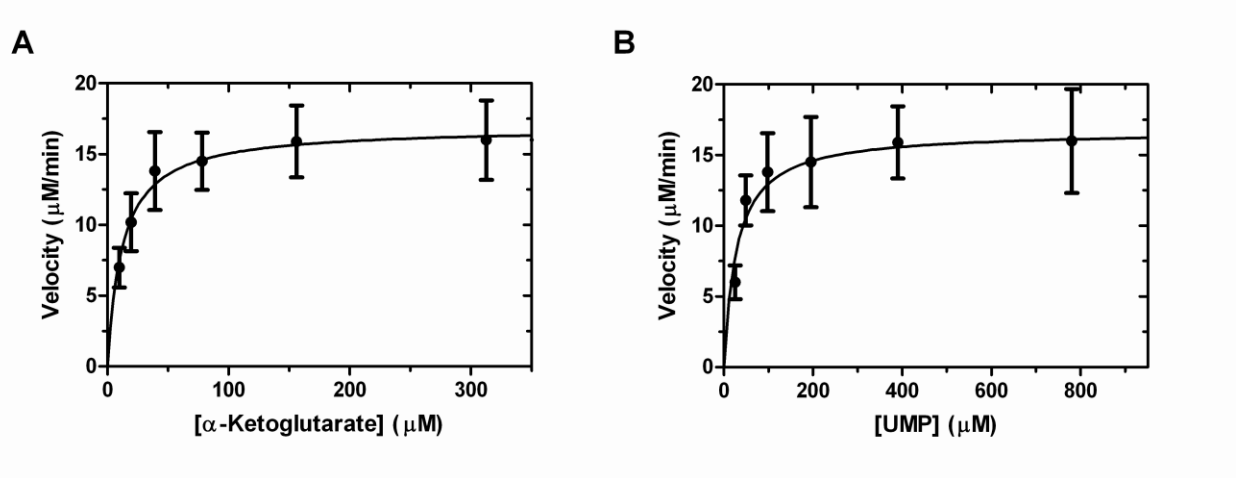

Fig. S13. Kinetic analysis of LipL using HPLC to detect product formation. (*A*) Single-substrate kinetic analysis using variable α-KG (9 μM-315 μM), near saturating UMP (2 mM), and 200 nM LipL. The extracted kinetic constants are K_m = 12 ± 3 μM and k_{cat} = 84 ± 18 min^{-1} . (*B*) Single-substrate kinetic analysis using variable UMP (25 μM-800 μM), near saturating α-KG (1 mM), and 200 nM LipL. The extracted kinetic constants are K_m = 28 ± 6 μM and k_{cat} = 81 ± 20 min^{-1} with respect to UMP. Data represent the average of two independent replicates obtained using end point assays under initial velocity conditions; S.E. was < 22% in all cases.

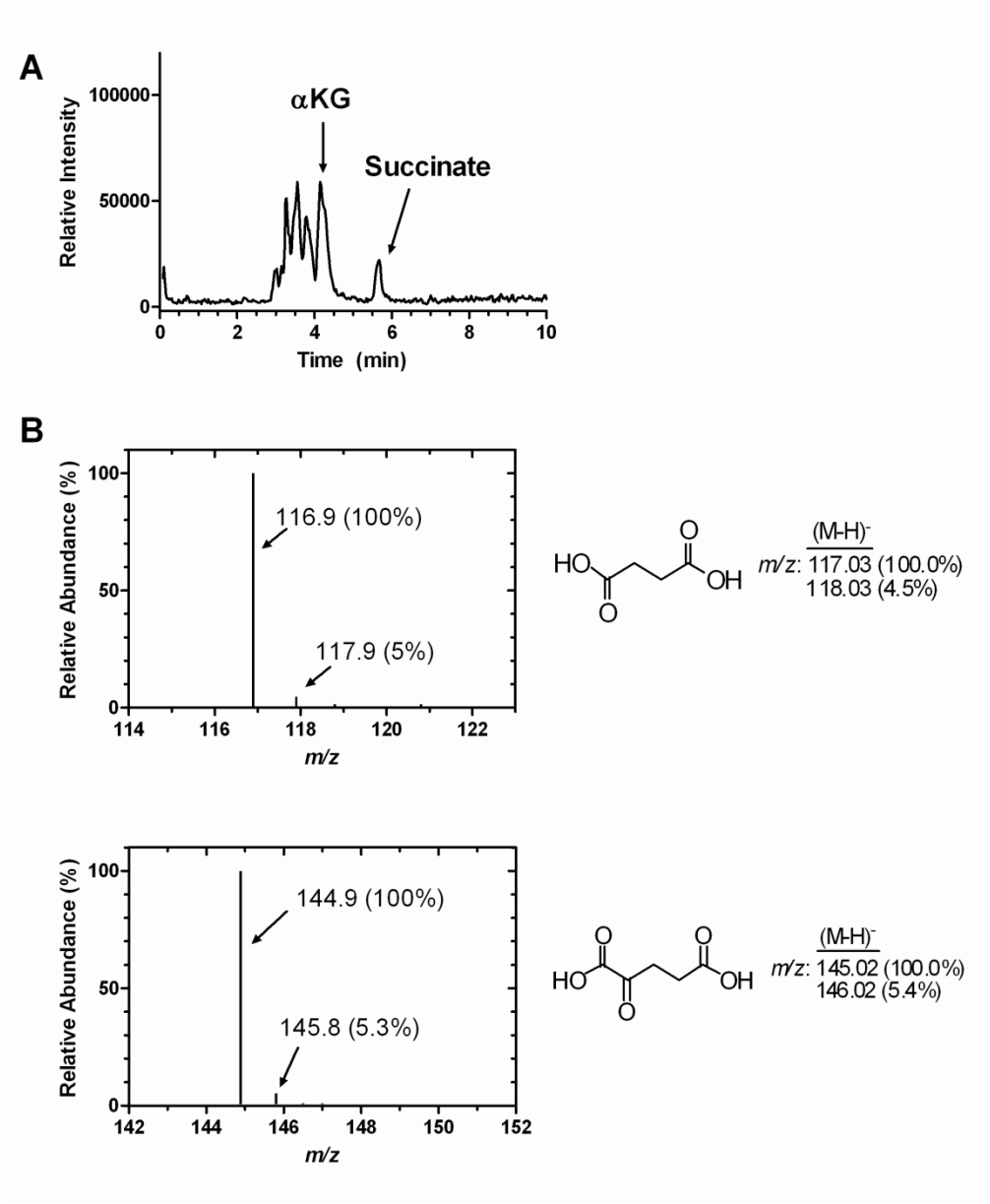

Fig. S14. LC-MS analysis of LipL activity without UMP. (*A*) The reaction components were detected by total negative ion current. (*B*) Mass spectrum for the peak at elution time t = 5.6 min corresponding to succinate and elution time t = 4.2 min corresponding to α-KG.

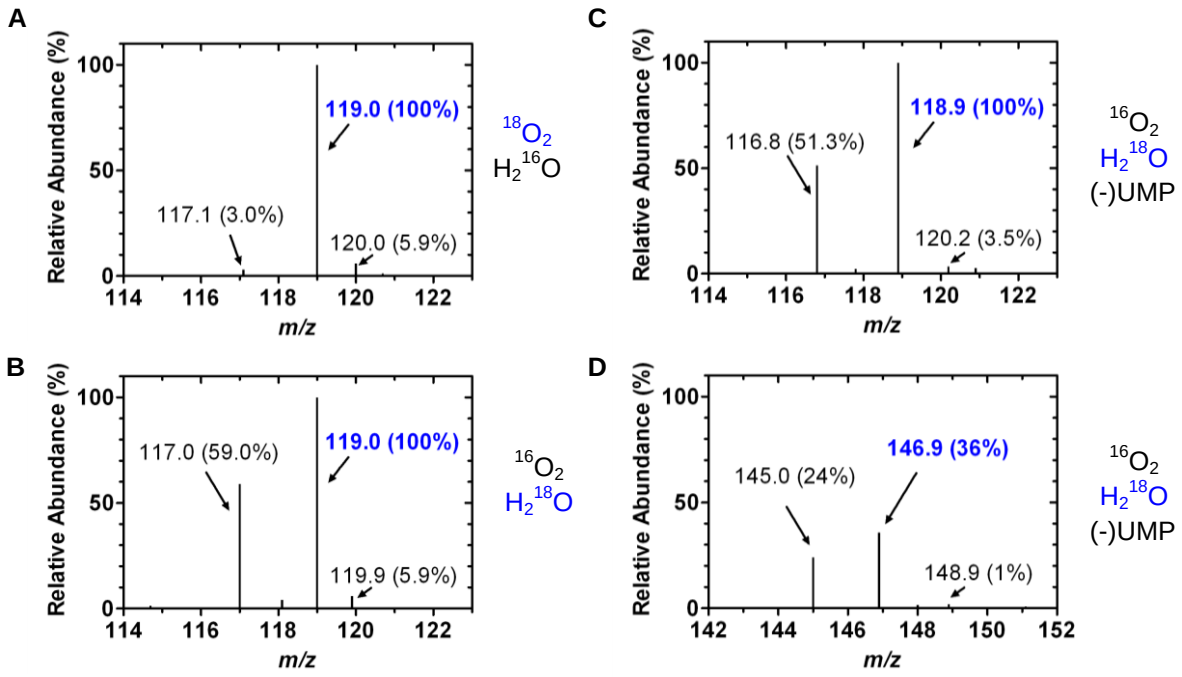

Fig. S15. Isotopic enrichment experiments. (*A*) Mass spectrum for the peak at elution time t = 5.6 min corresponding to succinate from a reaction performed in $^{18}O_2$. (*B*) Mass spectrum for the peak at elution time t = 5.6 min corresponding to succinate from a reaction performed in $H_2{}^{18}O$. (*C*) Mass spectrum for the peak at elution time t = 5.6 min corresponding to succinate from a reaction performed in $H_2{}^{18}O$ without UMP. (*D*) Mass spectrum for the peak at elution time t = 4.2 min corresponding to remaining α-KG from a reaction performed in $H_2{}^{18}O$ without UMP.

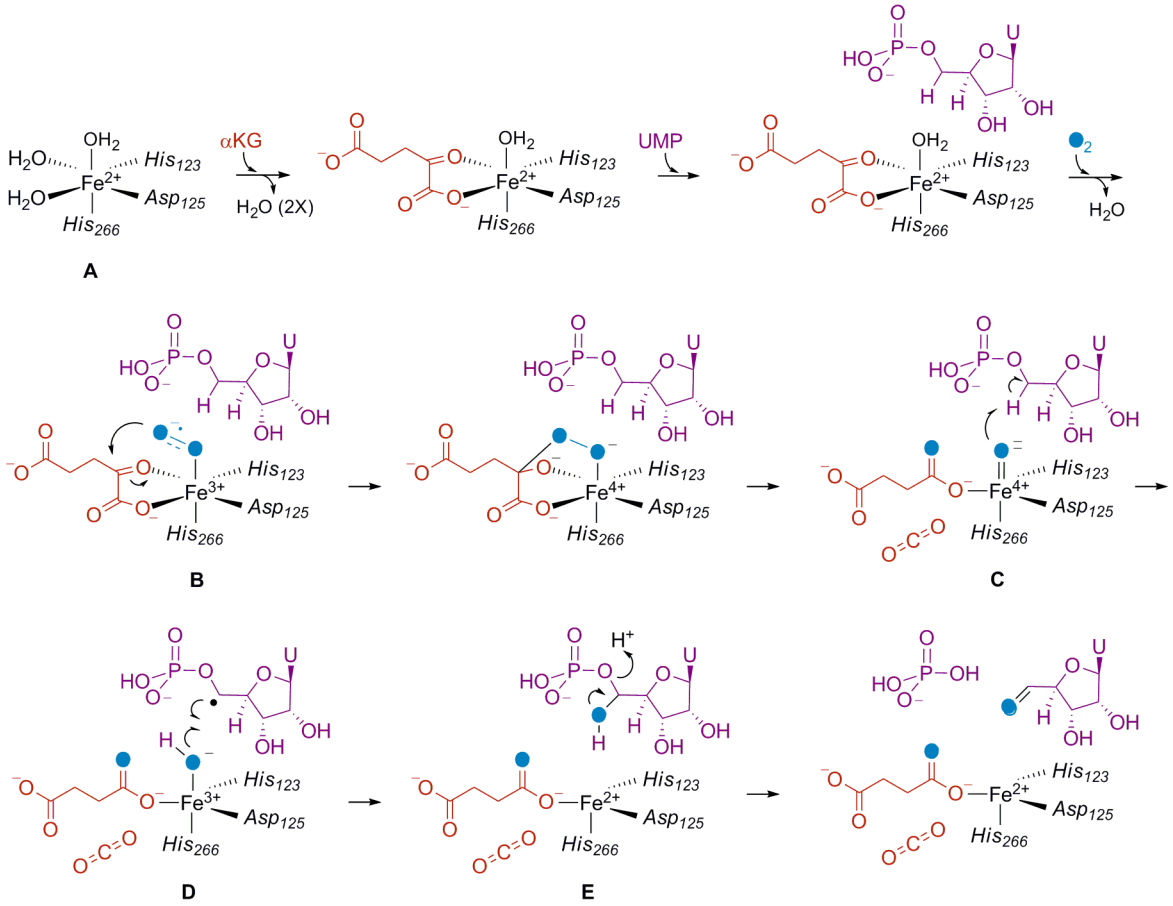

Fig. S16. Potential mechanism for LipL, an Fe(II)-dependent α–KG:UMP dioxygenase. In this mechanism, Fe(II) bind to form the holo-protein **A**, followed by an ordered sequential binding of α-KG and UMP, the latter of which leads to a substantial conformational change permitting dioxygen binding at the mononuclear center to form an Fe(III)-superoxo species **B**. Following the formation of **B**, the reaction proceeds with attack of the distal (uncoordinated) oxygen on the α-keto group of the bidentate-coordinated α-KG, which results in decarboxylation and O-O bond cleavage to form succinate, CO_2, and a high spin Fe(IV)-oxo intermediate **C**. Subsequently, the C-5' hydrogen of UMP is abstracted to form a carbon-centered radical and a Fe(III)-hydroxo center **D**, and the proximity of these two species results in oxygen rebound to yield 5'-hydroxy-5'-phosphouridine and a distorted Fe(II) center **E**, the former of which undergoes spontaneous phosphate elimination to yield the uridine-5'-aldehyde. Amino acids are numbered using the LipL sequence and are depicted as coordinating the iron based on the orientation within the TauD structure.

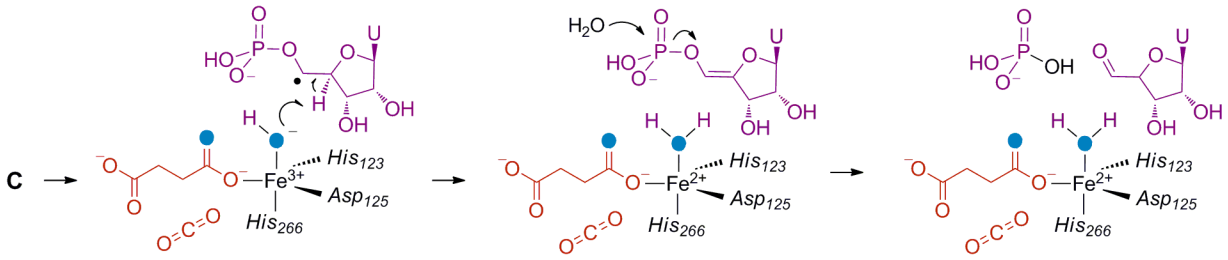

Fig. S17. Hypothetical partial mechanism for LipL, an Fe(II)-dependent α–KG:UMP dioxygenase. In this reaction mechanism starting from intermediate **C**, both the C-5' and C-4' hydrogens are removed in a desaturase-type mechanism, which is followed by dephosphorylation and tautomerization to yield the final product. Amino acids are numbered using the LipL sequence and are depicted as coordinating the iron based on the orientation within the TauD structure.

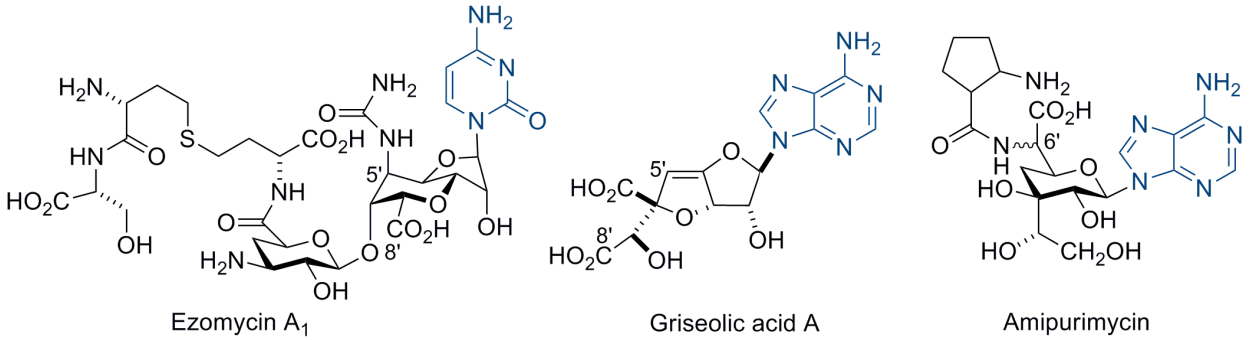

Fig. S18. High-carbon nucleosides whose biosynthesis may include an activity similar to LipL.